Retraining-Free Blockage Prediction for Millimeter-Wave Communications Based on Minor Components of Angular Power Profiles

Xiaoqing Tong*, Kohei Mitani*, Kazunori Hayashi*, Koji Yamamoto†, Takuto Arai‡,
Shuki Wai‡, Tatsuhiko Iwakuni‡, and Daisei Uchida‡
* Graduate School of Informatics, Kyoto University, Japan
† Department of Information and Human Science, Kyoto Institute of Technology, Japan
‡ NTT Access Network Service Systems Laboratories, Japan

***Abstract*—The paper proposes a retraining-free blockage prediction scheme that exploits angular power profiles (APPs) enabling us to proactively control system parameters of millimeter-wave (mmWave) communications systems. Specifically, we propose a feature extraction method using some minor components obtained by the principal component analysis (PCA) of the sample covariance matrix of APPs. Moreover, to cope with environmental changes without model retraining, we employ a vector database indexed by the feature vectors of the minor components as the machine learning model, and perform prediction of the obstacle positions and received signal-to-noise ratio (SNR) via a nearest-neighbor search of the database. Numerical experiments using measured APPs from an indoor mmWave communication environment demonstrate that the proposed method achieves prediction accuracy comparable to that of a supervised model using LightGBM, while the proposed approach does not require any retraining. Moreover, we confirm that prediction accuracy is preserved even when the database contains data from multiple environments with different obstacle velocities.**

I. Introduction

To realize high-speed, low-latency wireless links, the use of the 30-300 GHz millimeter-wave (mmWave) band is being investigated. Although the mmWave band can provide an extremely wide bandwidth, mmWave communications are vulnerable to blockages due to high straightness and a large path loss in propagation, compared to conventional microwave-band communications [1]–[3].

To cope with the blockages in mmWave communications, two countermeasure approaches have been investigated: the reactive approach, which detects an obstruction and then triggers control actions for the base station or user equipment, and the proactive approach, which anticipates a blockage and performs control in advance. Compared to the proactive approach, the reactive approach has the advantage of easier control and includes high-speed session transfer [4] and access point (AP) handover mechanisms [5]. However, with the approach, a drop in received signal power for some period resulting in packet loss and/or reduced throughput is unavoidable because a certain interval elapses between the onset of a blockage and the completion of the corresponding control procedure. To address this issue, several proactive methods have been proposed that augment mmWave systems with image sensors and take advantage of visual information to predict future blockages in advance [6]–[8]. However, the installation of image sensors not only increases system cost, but may also raise privacy concerns in the operating environment. Consequently, increasing attention has been paid to schemes that predict blockages by exploiting information contained in the received wireless signal itself, such as a method based on the received signal strength indicator (RSSI) [9] and a prediction scheme using the receiver side angle power profile (APP) obtained by beam search [10]. The APP-based schemes can achieve better accuracy than the RSSI based methods, since they utilize per-beam power measurements, which are supposed to have more information on the environment. Based on the idea, methods have been proposed that use APPs obtained both at the transmitter and the receiver [11], and that combine APPs with acoustic signals generated by obstacles [12].

Prior studies that exploited APPs [10]–[12] have predicted future blockages by directly using the measured raw profile as input. If we consider a situation just before a blockage, the APP would contain both the LOS component and the obstacle-reflected components. The components of the reflected waves will be beneficial for the blockage prediction, but the LOS power overwhelms the reflections, and thus, if we directly use APPs, the information carried by the reflected wave could be masked, which can hinder effective learning.

Moreover, existing methods relying on RSSI [9] or APPs [10]–[12] typically employ supervised machine learning models to predict the blockage. Because the prediction models are environment dependent and the wireless channel environment changes with the terminal position or some other reasons, the model parameters must be retrained whenever the environment changes. In practice, however, the computational cost and latency of retraining can be prohibitive, making the need for retraining a major obstacle to the practical implementation in wireless communication systems.

In this paper, to suppress the LOS contribution and highlight the reflection component, we propose to construct a feature vector using some minor components obtained by the principal

979-8-3315-7206-8/25/$31.00

component analysis (PCA) [13] of the sample correlation matrix of APPs. Since principal components would correspond to the LOS path and minor components to the reflected paths, the prediction performance could be enhanced using the proposed feature vector. Moreover, to eliminate the need for retraining and enable rapid adaptation to environmental changes, we employ the vector database as a machine learning model as in [14] and store the feature vector (key) with the corresponding value to be predicted, such as the future obstacle position or the future received signal-to-noise ratio (SNR) in the database. The blockage prediction can then be performed by the nearest neighbor search of the database. During operation, the feature vector representing the current environment and corresponding value are added to the database, enabling adaptation to time-variant environments without retraining. Numerical experiments using measured APPs from an indoor mmWave communication environment demonstrate that the proposed method achieves prediction accuracy comparable to that of a supervised model using LightGBM [15], while the proposed approach does not require any retraining. Moreover, we confirm that prediction accuracy is preserved even when the database contains data from multiple environments with different obstacle velocities.

II. Measurement Environment

As illustrated in Fig. 1, measurements have been conducted in an indoor environment with a room of approximately $7\ \mathrm{m} \times 6\ \mathrm{m}$, where two mmWave radio stations (AP and STA) are installed facing each other.

During the measurements, an obstacle was moving inside a designated target area between the stations, where the target areas were defined as a $2.5\ \mathrm{m} \times 2.5\ \mathrm{m}$ square region for the case with trajectory 1 and a $1.5\ \mathrm{m} \times 1.5\ \mathrm{m}$ square region for trajectory 2. A human subject with aluminum foil wrapped around the waist served as the obstacle and moved within the target area at two different moving speeds: $0.25\ \mathrm{m/s}$ and $0.5\ \mathrm{m/s}$. During the obstacle movement, the STA has continuously transmitted mmWave signals to the AP using a fixed directional beam with a half-power beamwidth of 16 degrees. On the other hand, the AP has repeatedly performed beam scans with 33 beams at every 21 ms resulting, for each scan, in a received SNR vector of size 33×1, where each elemThe received SNR vector at time t is defined as

$$\boldsymbol{s}_t = \begin{pmatrix} s_{t,1} & s_{t,2} & \cdots & s_{t,33} \end{pmatrix}^\top \in \mathbb{R}^{33}, \tag{1}$$

where $(\cdot)^\top$ denotes the transpose. Note that, to suppress fluctuations in the observed SNR due to measurement noise, we have applied HMM-GMM model-based smoothing proposed in [12] to the received SNR vector.

Examples of obstacle movement trajectories for the moving speed of $0.25\ \mathrm{m/s}$ are shown in Fig. 2, where approximately 26,000 samples were collected on trajectory 1 and 8,000 samples on trajectory 2 using a position tracker. For the moving speed of $0.5\ \mathrm{m/s}$, about 26,000 samples were collected on trajectory 1 and 4,000 on trajectory 2. In addition, approximately 18,000 "null" samples were obtained without any obstacle

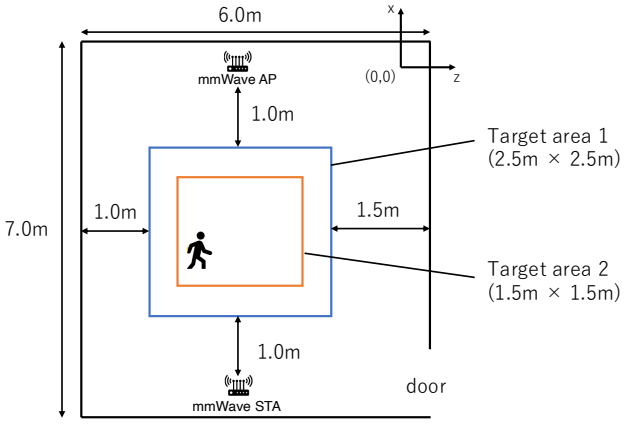

Fig. 1: Measurement Environment

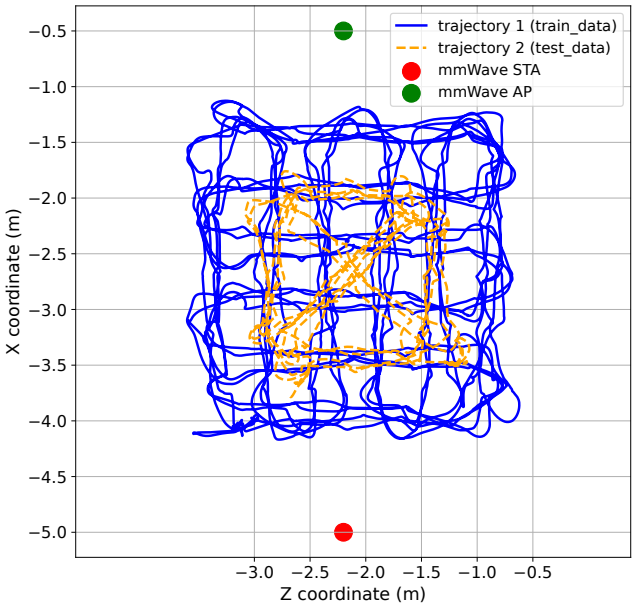

Fig. 2: Examples of obstacle movement trajectories at 0.25m/s obtained by using a position tracker

present. In subsequent analysis, the data measured on trajectory 1 are used as training data, the data on trajectory 2 as test data, and the null samples to build the correlation matrix. Also, we distinguish corresponding received SNR vectors with the superscripts as $\boldsymbol{s}_t^{\mathrm{Tr}}$, $\boldsymbol{s}_t^{\mathrm{Ts}}$, and $\boldsymbol{s}_t^{\mathrm{Nu}}$, respectively.

III. Proposed Feature-Vector Generation Based on Minor Components

A. Motivation

A typical received SNR vector observed in the absence of blockage due to the obstacle is illustrated in Fig. 3. Since the directional beam with index 17 is precisely oriented toward the transmitter (STA), it can capture the direct LOS wave efficiently and thus the SNR vector exhibits a peak at index 17. In contrast, it has been shown in [12] that the reflected

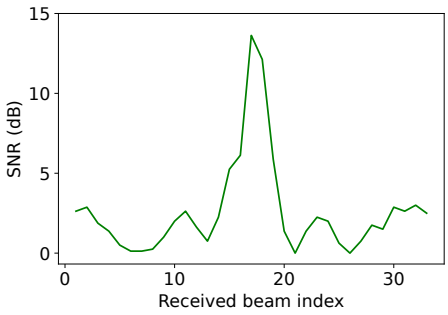

Fig. 3: Example of typical SNR vector in the absence of obstacle

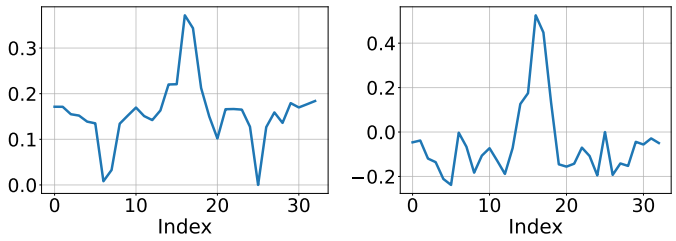

(a) 1st principal component (b) 2nd principal component

Fig. 4: Eigenvector profiles

waves at the obstacle arrive from directions slightly offset to either side of the LOS direction, when a moving obstacle is about to block the LOS path. Consequently, more accurate blockage prediction could be possible by focusing on signals arriving from either side of the LOS direction, rather than the LOS direction, and extracting them appropriately. To this end, we assume that the principal components of the SNR vector with greater contributions originate from the LOS component, and we investigate the extraction of a feature vector for future blockage prediction by using the principal components with smaller contributions, namely the minor components.

B. Principal Component Analysis of Received SNR Vector

To perform PCA of the received SNR vectors, we firstly compute the sample correlation matrix of the SNR vectors as

$$\boldsymbol{\Sigma} = \frac{1}{N-1}\sum_{t=1}^{N}(\boldsymbol{s}_t^{\mathrm{Nu}} - \boldsymbol{\mu})(\boldsymbol{s}_t^{\mathrm{Nu}} - \boldsymbol{\mu})^{\top}, \tag{2}$$

where N denotes the total number of SNR vectors used for the computation of the sample correlation matrix, and

$$\boldsymbol{\mu} = \frac{1}{N}\sum_{t=1}^{N}\boldsymbol{s}_t^{\mathrm{Nu}} \tag{3}$$

is the sample mean of the SNR vectors.

Then, we perform eigenvalue decomposition of the sample correlation matrix as

$$\boldsymbol{\Sigma} = \boldsymbol{U}^{\top}\boldsymbol{\Lambda}\boldsymbol{U}, \tag{4}$$

$$\boldsymbol{\Lambda} = \mathrm{diag}\begin{pmatrix}\lambda_1 & \lambda_2 & \cdots & \lambda_{33}\end{pmatrix}, \tag{5}$$

$$\boldsymbol{U} = \begin{pmatrix}\boldsymbol{u}_1 & \boldsymbol{u}_2 & \cdots & \boldsymbol{u}_{33}\end{pmatrix}, \tag{6}$$

where $\mathrm{diag}(\boldsymbol{a})$ denotes a diagonal matrix with the components of a vector $\boldsymbol{a}$ as diagonal elements, λ_i $(i = 1, 2, \ldots, 33)$ represents the eigenvalues of $\boldsymbol{\Sigma}$ with descending order, and $\boldsymbol{u}_i$ is the eigenvector corresponding to λ_i.

Note that we have used the data observed in the absence of obstacles (null data) for the computation of the sample correlation matrix. Since the signal contained in the null data is primarily attributed to the direct path, using null data ensures that the principal components with higher contribution contain only the direct wave. Fig. 4 shows the profiles of the eigenvectors corresponding to the first and second eigenvalues. As shown in the figure, the shapes of the dominant principal components exhibit peaks at beam index 17. Moreover, the shapes of the principal components closely resemble that of the SNR vector shown in Fig. 3, supporting the hypothesis that "principal components with higher contribution rates are attributed to the direct wave."

C. Proposed Feature Vector Generation Method

Based on the discussions in Sections III-A and III-B, in the proposed method, we construct feature vectors by eliminating the contributions of the eigenvectors corresponding to the n largest eigenvalues of the sample correlation matrix from the received SNR vectors in the training data.

Specifically, we define a matrix composed by $33 - n$ eigenvectors corresponding to $33 - n$ minor components as

$$\overline{\boldsymbol{U}} = \begin{pmatrix}\boldsymbol{u}_{n+1} & \boldsymbol{u}_{n+2} & \cdots & \boldsymbol{u}_{33}\end{pmatrix}, \tag{7}$$

and generate feature vectors by the projection given by

$$\overline{\boldsymbol{s}}_t^{\mathrm{Tr}} = \overline{\boldsymbol{U}}\left(\overline{\boldsymbol{U}}^{\top}\overline{\boldsymbol{U}}\right)^{-1}\overline{\boldsymbol{U}}^{\top}\boldsymbol{s}_t^{\mathrm{Tr}}. \tag{8}$$

IV. Proposed Prediction Method Using Vector Database

A. Database Construction

The database is constructed using the training data following a unified key-value structure. The key vector $\overline{\boldsymbol{S}}_t$ at time t is defined as a stacked vector of feature vectors generated from received SNR vectors observed from time $t - w + 1$ to t with w time steps (1 time step = 21 ms) as

$$\overline{\boldsymbol{S}}_t = \begin{pmatrix}\overline{\boldsymbol{s}}_{t-w+1}^{\mathrm{Tr}\top} & \overline{\boldsymbol{s}}_{t-w+2}^{\mathrm{Tr}\top} & \cdots & \overline{\boldsymbol{s}}_t^{\mathrm{Tr}\top}\end{pmatrix}^{\top} \tag{9}$$

The value y_t associated with each key vector varies depending on the specific task. Although the main purpose of the paper is the blockage prediction, we consider not only the received SNR prediction but also the position estimation and prediction of the obstacle in order to understand the capability of the proposed approach. Specific value y_t for each task is as follows:

- **Position estimation:** $y_t = z_t$ (z_t denotes the z-axis coordinate of the obstacle at time t)
- **Position prediction:** $y_t = z_{t+a}$ (z-axis coordinate of the obstacle at time $t + a$ with $a > 0$)

- **Received SNR prediction:** $y_t = s^{\mathrm{Tr}}_{t+a,17}$ (the 17th element of the received SNR vector at time $t+a$ with $a > 0$)

For the position-related tasks, we focus only on the z-axis coordinate because, in the channel environment of the study, the movement in the z-axis direction primarily affects blockage, whereas the obstacle moves in two-dimensional coordinates.

For each task, we create pairs $\boldsymbol{D}_t = \left(\overline{\boldsymbol{S}}_t, y_t\right)$ that link keys and values, and store them in the database as

$$\mathcal{D} = \{\boldsymbol{D}_1, \boldsymbol{D}_2, \ldots, \boldsymbol{D}_M\}, \tag{10}$$

where M is the total number of training samples available for the specific task.

B. Query Vector Generation

The query vector is calculated using the test data in the same manner as the key vector generation. Specifically, the contributions of the direct path are eliminated by the projection on to the minor components as

$$\overline{\boldsymbol{s}}^{\mathrm{Ts}}_t = \overline{\boldsymbol{U}}\left(\overline{\boldsymbol{U}}^{\top}\overline{\boldsymbol{U}}\right)^{-1}\overline{\boldsymbol{U}}^{\top}\boldsymbol{s}^{\mathrm{Ts}}_t, \tag{11}$$

and the query vector is generated by stacking $\overline{\boldsymbol{s}}^{\mathrm{Ts}}_t$ as

$$\overline{\boldsymbol{Q}}_t = \left(\overline{\boldsymbol{s}}^{\mathrm{Ts}\top}_{t-w+1} \quad \overline{\boldsymbol{s}}^{\mathrm{Ts}\top}_{t-w+2} \quad \cdots \quad \overline{\boldsymbol{s}}^{\mathrm{Ts}\top}_{t}\right)^{\top}. \tag{12}$$

C. Estimation/Prediction using k-Nearest Neighbor Search

In the proposed method, we have employed standard k-nearest neighbor search using Euclidean distance

$$d\left(\overline{\boldsymbol{Q}}_t, \overline{\boldsymbol{S}}_t\right) = \left\|\overline{\boldsymbol{Q}}_t - \overline{\boldsymbol{S}}_t\right\|_2 \tag{13}$$

to find the k closest key vectors to the query $\overline{\boldsymbol{Q}}_t$. Using the search results, the estimation/prediction result is obtained by averaging the corresponding values as

$$\hat{y}(\overline{\boldsymbol{Q}}_t) = \frac{1}{k}\sum_{t' \in \mathcal{N}_k(\overline{\boldsymbol{Q}}_t)} y_{t'}, \tag{14}$$

where $\mathcal{N}_k(\boldsymbol{q}_t)$ denotes the index set of the k nearest neighbors.

V. Numerical Experiments

To demonstrate the performance of the proposed approach, we have conducted numerical experiments using measured data in the environment described in Sec. II. For performance evaluation, data obtained with an obstacle moving speed of 0.25 m/s have been used both for database construction and query generation with a window length of $w = 50$, except in Sec.V-D. As a baseline scheme, we have employed LightGBM as the supervised machine learning model for solving the estimation and prediction problems, where the input signal is generated with the same method as the proposed approach using the stacked feature vectors. In the learning process, the ideal outputs (ground truth) are set according to the same task-specific definitions, namely $y_t = z_t$ for position estimation, $y_t = z_{t+a}$ for position prediction, and $y_t = x_{t+a,17}$ for the received SNR prediction.

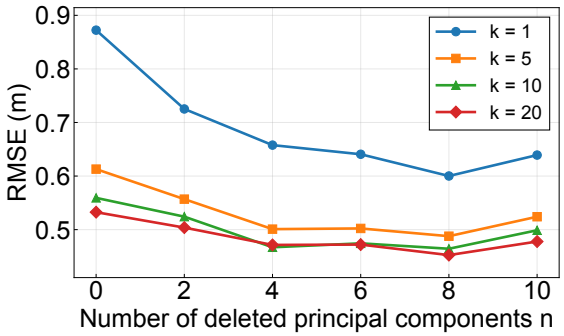

Fig. 5: RMSE performance of obstacle position estimation versus number of removed principal components n

TABLE I: RMSE of obstacle position estimation (m)

Machine Learning Model	RMSE
Database w/o proposed feature vectors (n=0, k=20)	0.53
Database with proposed feature vectors (n=8, k=20)	0.45
LightGBM w/o proposed feature vectors (n=0)	0.41
LightGBM with proposed feature vectors (n=8)	0.37

A. Obstacle Position Estimation

The obstacle position estimation performance has been evaluated by the root-mean-square error (RMSE) between the estimated and true coordinates. To assess the impact of removal of the principal components in the proposed method, Fig. 5 shows the RMSE performance of the obstacle position estimation with the proposed method versus the number of deleted principal components n with different numbers of nearest neighbor search $k \in \{1, 5, 10, 20\}$. From the figure, we can see that the RMSE performance can be improved with an appropriate choice of $n(\neq 0)$, which demonstrates the validity of the proposed feature generation method, and that the lowest RMSE is achieved at $n = 8$ for all k. Moreover, RMSE performance improves with larger k, presumably because a broader search mitigates error due to fluctuations of the values in the database.

To compare the performance of the proposed method with the existing supervised machine learning model, Table I shows the RMSEs of the proposed method using the database and the supervised LightGBM model with ($n = 8$) and without ($n = 0$) the proposed feature vector generation method. The results show that the proposed feature generation method using minor components is beneficial for LightGBM as well. Although some degradation can be recognized, the proposed method using the database can achieve RMSE comparable to LightGBM.

B. Obstacle Position Prediction

Fig. 6 shows the RMSE of obstacle position prediction with the proposed method versus the number of deleted principal components n with different number of nearest neighbor search $k \in \{1, 5, 10, 20\}$, where the prediction horizon is set to $a = 10$.

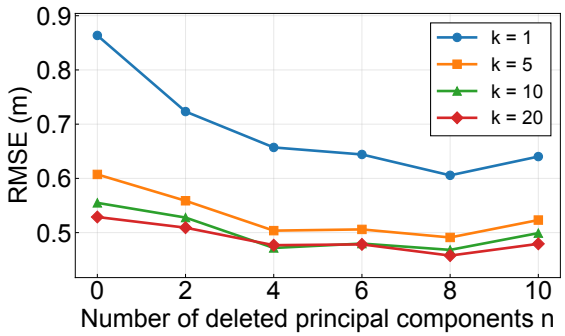

Fig. 6: RMSE performance of obstacle position prediction versus number of removed principal components n

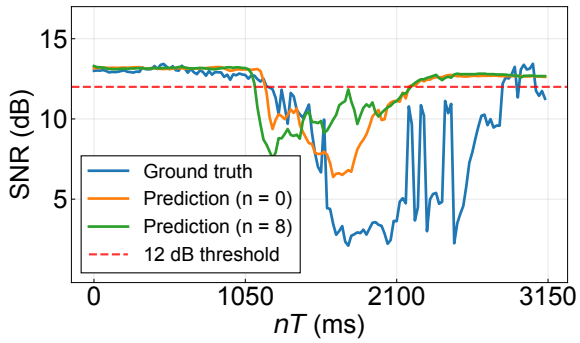

Fig. 7: Example of received SNR prediction (prediction horizon $a = 10$)

TABLE II: RMSE of obstacle position prediction (m)

Machine Learning Model	a=10	a=20	a=30
Database w/o proposed feature vectors (n=0, k=20)	0.53	0.53	0.52
Database with proposed feature vectors (n=8, k=20)	0.46	0.46	0.47
LightGBM w/o proposed feature vectors (n=0)	0.42	0.42	0.42
LightGBM with proposed feature vectors (n=8)	0.38	0.39	0.40

TABLE III: Average prediction lead time (steps) for received SNR drops

Machine Learning Model	a=5	a=10	a=15
Database w/o proposed feature vectors (n=0, k=20)	2.85	4.85	6.31
Database with proposed feature vectors (n=8, k=20)	3.62	6.77	9.08
LightGBM w/o proposed feature vectors (n=0)	4.31	7.85	10.08
LightGBM with proposed feature vector (n=8)	4.54	8.08	10.77

As in the case with the obstacle position estimation, the best RMSE is achieved with $n = 8$, and the larger k improves the RMSE.

Table II summarizes the RMSEs of the obstacle position prediction with the proposed database approach and the supervised LightGBM model with the prediction horizons of $a = 10$, 20, and 30 with ($n = 8$) and without ($n = 0$) the proposed feature vector generation method. Consistent with the obstacle position estimation results, the proposed feature vector generation method can reduce the RMSE for both models, and the proposed database model achieves the RMSE close to that of LightGBM.

C. Received SNR Prediction

To obtain the first indication of the effectiveness of the proposed feature vector generation method for the prediction of the received SNR with the beam index of 17, Fig. 7 shows an example of the prediction results, where the blue curve represents the true received SNR with the beam index of 17, and the orange and green curves show the prediction results with $n = 0$ and $n = 8$, respectively. In the prediction task, the prediction horizon is set to $a = 10$ and $k = 10$ is used for the nearest neighbor search. From the figure, we can see that the proposed feature vector generation method ($n = 8$) can achieve an earlier prediction of the SNR drop, while the predicted received SNRs after the SNR drop are quite different from the ground truth. Note here that, from the perspective of proactive system control to avoid communication outage, what matters is how much in advance the SNR drop can be predicted, since the larger the lead time, the more margin is available for the control. Consequently, we evaluate the prediction lead time for the SNR drop, which is defined as the event that the received SNR falls below 12 dB, as the performance measure for the received SNR prediction task.

Table III summarizes the average prediction lead times in steps of the proposed database method and the supervised LightGBM model with and without the proposed feature vector generation method, where the prediction horizons are set to $a = 5$, 10, and 15. As in the obstacle position estimation and prediction tasks, the proposed feature vector generation method can improve the performance in terms of the average lead time of both models as well. Moreover, the proposed database method can achieve an average lead time comparable to that of LightGBM.

D. Sensitivity to mismatch database

Finally, to evaluate the sensitivity of the proposed approach to the mismatch between the training data and the test data, we construct three different databases using data obtained with two different moving speeds of obstacle 0.25 m/s and 0.5 m/s as follows:

- D_1: contains data of both 0.25 m/s and 0.5 m/s
- D_2: contains data of 0.25 m/s only
- D_3: contains data of 0.5 m/s only

For the generation of feature vectors from the data with 0.25 m/s, the number of deleted principal components is set to $n = 8$, while it is set to $n = 10$ for the data with 0.5 m/s based on numerical evaluations. The number of neighbors k in the nearest neighbor search is chosen individually for each case to give the best prediction performance in the following analysis.

TABLE IV: RMSE of obstacle position prediction (m) with different databases ($a = 10$)

Database	Query: 0.25 m/s	Query: 0.5 m/s
D_1 (**0.25 m/s + 0.5 m/s**)	0.48	0.50
D_2 (**0.25 m/s**)	0.46	0.54
D_3 (**0.5 m/s**)	0.60	0.50

TABLE V: Average prediction lead time (steps) for received SNR drops with different databases ($a = 10$)

Database	Query: 0.25 m/s	Query: 0.5 m/s
D_1 (**0.25 m/s + 0.5 m/s**)	7.23	6.17
D_2 (**0.25 m/s**)	6.77	5.75
D_3 (**0.5 m/s**)	6.46	6.00

Obstacle Position Prediction: The obstacle position prediction is performed for the data with $0.25\ \mathrm{m/s}$ and $0.50\ \mathrm{m/s}$ by using databases D_1, D_2, and D_3, where e the prediction horizon is set to $a = 10$. The RMSE performance is summarized in Table IV. From the results, we can confirm that, even when two different environments are stored together in the database ($\mathcal{D}_1$), the prediction can be made without a significant performance loss.

Received SNR Prediction: Table V shows the average lead time for the received SNR drop for the data with $0.25\ \mathrm{m/s}$ and $0.50\ \mathrm{m/s}$ by using databases D_1, D_2, and D_3, where the prediction horizon is set to $a = 10$. From the results, it is confirmed that the prediction of the received SNR drop can be performed without a decrease in the lead time even when the database stores data from two different environments.

VI. Conclusions

We have investigated a method for generating feature vectors from angular power profiles to predict blockage caused by a moving obstacle in mmWave wireless communications systems. As an approach without the need for retraining machine learning models even when the environment changes, we have examined a blockage prediction method using a vector database. Moreover, we have proposed a feature vector generation method by extracting minor components of the received SNR vectors. The performance of the proposed approach is evaluated with the tasks of the obstacle position estimation/prediction the and received SNR prediction, confirming the effectiveness of the proposed feature vector generation method not only for the proposed model with the databases but also for the supervised LightGBM model. Moreover, we have confirmed that the proposed feature vector and database-based method achieves prediction performance comparable to that of supervised LightGBM model. In addition, the robustness of the proposed approach against the mismatch database is confirmed by the numerical experiment using data with different obstacle speeds. The results show that prediction is possible without performance degradation even when a database containing data from two different environments is used.

Future work includes direct control of system parameters based on the measured APPs to cope with blockage of the LOS path.

The present study is limited to a single indoor environment with a fixed layout and a single moving obstacle. Although it shows robustness to obstacle velocity, further validation in varied room configurations and with multiple moving or stationary obstacles is needed to confirm generalization.

References

[1] T. Bai and R. W. Heath, "Coverage and rate analysis for millimeter-wave cellular networks," *IEEE Transactions on Wireless Communications*, vol. 14, no. 2, pp. 1100–1114, 2015.

[2] S. Collonge, G. Zaharia, and G. Zein, "Influence of the human activity on wide-band characteristics of the 60 ghz indoor radio channel," *IEEE Transactions on Wireless Communications*, vol. 3, no. 6, pp. 2396–2406, 2004.

[3] A. Yamamoto, K. Ogawa, T. Horimatsu, A. Kato, and M. Fujise, "Path-loss prediction models for intervehicle communication at 60 ghz," *IEEE Transactions on Vehicular Technology*, vol. 57, no. 1, pp. 65–78, 2008.

[4] E. Perahia and M. X. Gong, "Gigabit wireless lans: an overview of ieee 802.11ac and 802.11ad," *SIGMOBILE Mob. Comput. Commun. Rev.*, vol. 15, no. 3, pp. 23–33, Nov. 2011. [Online]. Available: https://doi.org/10.1145/2073290.2073294

[5] B. Gao, Z. Xiao, C. Zhang, L. Su, D. Jin, and L. Zeng, "Double-link beam tracking against human blockage and device mobility for 60-ghz wlan," in *2014 IEEE Wireless Communications and Networking Conference (WCNC)*, 2014, pp. 323–328.

[6] T. Nishio, H. Okamoto, K. Nakashima, Y. Koda, K. Yamamoto, M. Morikura, Y. Asai, and R. Miyatake, "Proactive received power prediction using machine learning and depth images for mmwave networks," *IEEE Journal on Selected Areas in Communications*, vol. 37, no. 11, pp. 2413–2427, 2019.

[7] G. Charan, M. Alrabeiah, and A. Alkhateeb, "Vision-aided dynamic blockage prediction for 6g wireless communication networks," in *2021 IEEE International Conference on Communications Workshops (ICC Workshops)*, 2021, pp. 1–6.

[8] M. Alrabeiah, A. Hredzak, and A. Alkhateeb, "Millimeter wave base stations with cameras: Vision-aided beam and blockage prediction," in *2020 IEEE 91st Vehicular Technology Conference (VTC2020-Spring)*, 2020, pp. 1–5.

[9] S. Wu, M. Alrabeiah, A. Hredzak, C. Chakrabarti, and A. Alkhateeb, "Deep learning for moving blockage prediction using real mmwave measurements," pp. 3753–3758, 2022.

[10] A. Alkhateeb, I. Beltagy, and S. Alex, "Machine learning for reliable mmwave systems: Blockage prediction and proactive handoff," in *2018 IEEE Global Conference on Signal and Information Processing (GlobalSIP)*, 2018, pp. 1055–1059.

[11] I. Yonemura, T. Kanda, R. Hanahara, K. Yamamoto, T. Arai, S. Wai, T. Iwakuni, D. Uchida, and N. Kita, "Blockage prediction using exhaustive beam-pair scan in mmwave networks: An experimental study," in *2023 IEEE 20th Consumer Communications & Networking Conference (CCNC)*, 2023, pp. 309–312.

[12] R. Hanahara, I. Yonemura, K. Yamamoto, T. Arai, S. Wai, T. Iwakuni, D. Uchida, and N. Kita, "Leveraging acoustic aoa to enhance mmwave beam search-based blockage prediction: An experimental study," *IEEE Transactions on Vehicular Technology*, vol. 73, no. 10, pp. 15 598–15 608, 2024.

[13] I. T. Jolliffe and J. Cadima, "Principal component analysis: a review and recent developments," *Philosophical transactions of the royal society A: Mathematical, Physical and Engineering Sciences*, vol. 374, no. 2065, 2016.

[14] D. Li, B. Zhang, Z. Yao, and C. Li, "A feature scaling based k-nearest neighbor algorithm for indoor positioning system," in *2014 IEEE Global Communications Conference*, 2014, pp. 436–441.

[15] G. Ke, Q. Meng, T. Finley, T. Wang, W. Chen, W. Ma, Q. Ye, and T.-Y. Liu, "Lightgbm: A highly efficient gradient boosting decision tree," in *Advances in neural information processing systems (NIPS)*, vol. 30, 2017, pp. 3149–3157.